

INTERACTION EFFECT OF OPERATING PARAMETERS DURING OXIDATION OF DIFFERENT DYES VIA THE FENTON PROCESS. APPLICATION OF THE PLACKETT-BURMANN DESIGN

Imene Djeghader^{1,2, ✉}, Farida Bendebane^{1,3}, Fadhel Ismail^{1,2}

<https://doi.org/10.23939/chcht17.01.154>

Abstract. The interaction effect of eight operating factors on the degradation of three organic dyes of different structures (Cibacron green, methylene blue and methyl orange) has been studied. Effect had been evaluated statistically using the Plackett-Burman screening design which extracted valuable information on the most important parameters and their interactions. The goodness of the model fit was checked by the determination of the coefficient R^2 . The process factors, which affected the degradation efficiency of dyes, were then analyzed and illustrated; the most important values (p and F) for three dyes proved the validity of the model. The results of interactions between the factors allow to understand and study the impact of each parameter on the elimination of dyes and to distinguish the key factor to upgrade the efficiency of the Fenton process.

Keywords: Fenton oxidation, dyes removal, water treatment, design of experiment, ANOVA analysis.

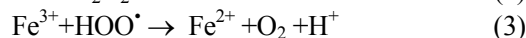
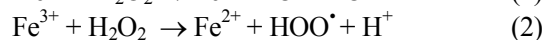
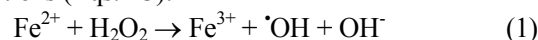
1. Introduction

The drainage of industrial effluents in textile, tannery or printing factories often presents a polluting discharge that is difficult to biodegrade. The conventional treatments currently used are not very reliable and no longer meet the requirements of environmental protection. Over the past two decades, advanced oxidation treatment has proven to be a promising new technology for the degradation of many toxic and poorly biodegradable organic pollutants.

The Fenton reaction, which involves hydroxyl radicals as the primary oxidants, is one of the most useful

oxidation processes that can effectively degrade various substrates. Although more than a century Henry JH Fenton^{1,2} discovered the oxidation of polyhydric alcohols and organic acids during the reaction between Fe(II) and H_2O_2 ; it is only in recent decades that much more researches have been carried out so far on the Fe^{2+}/H_2O_2 system, whether at the level of the interaction mechanism^{3,4} or at the level of applications in the oxidation system of organic pollutants in an aqueous medium,⁵⁻⁷ as well as for different types of water: drinking water,⁸ explosives discharges.^{9,10} The main advantage of the Fenton treatment is the complete destruction of contaminants into harmless compounds such as carbon dioxide, water and inorganic salts. The Fenton reaction causes the oxidant dissociation and the formation of highly reactive hydroxyl radicals ($\cdot OH$) which attack and destroy organic pollutants.¹¹

Depending on the structure of the organic compound, the hydroxyl radical can react with unsaturated compounds (vinylics and aromatics) more easily and faster than aliphatic compounds.^{12,13} The classic description of the traditional Fenton treatment is based on three main reactions (Eqs.1-3).¹⁴



Although Fenton oxidation is mostly described by above-mentioned simple steps (Eqs.1-3), the process is more complex, as it includes many other interactions. Generally, these processes can be regrouped into initiation, propagation, and termination reactions.¹⁵

Cibacron green (CG), methylene blue (MB) and methyl orange (MO) are three dyes found mainly in industrial effluents; The CG is an azo dye which poses a real problem of water contamination due to the activity of local industries. According to the literature, its degradation has been a bit studied. MB is one of the cationic dyes widely used in the dyeing of several supports, in particular silk, cotton, wood and for the temporary coloring of paper,^{16,17} as well as in the chemical, biological and medical

¹ LOMOP Research Laboratory, Badji Mokhtar University of Annaba, Annaba, 23000, Algeria

² Department of Process Engineering, Badji Mokhtar University of Annaba, Annaba, 23000, Algeria

³ Department of Chemistry, Badji Mokhtar University of Annaba, Annaba, 23000, Algeria

✉ nourdjeghader@gmail.com

© Djeghader I., Bendebane F., Ismail F., 2023

fields. MO is an azo dye chosen as a representative model of anionic organic pollutants because it is one of the well-known weak acids and widely used in the paper, printing, textile and pharmaceutical industries;¹⁷ its modest biodegradability has attracted the attention of scientists in the environmental field. Therefore, the removal of these dyes from wastewater is necessary for human and environmental health. For many process optimization problems in industries, the interactions between factors are of great concern to many researchers, so they must be properly investigated. The root cause of the problem is sometimes due to the interaction between the factors rather than the individual effect of each factor in response.¹⁸ To specify the nature of an interaction, it is necessary to determine the effect of each factor for various conditions of other factors. However, we have to look for more information obtained gradually and clearly with a minimum of experiments and with very small errors. The simplest way to solve this problem is to use a fractional "Plackett-Burman" factorial design, in which two levels are chosen for each factor. The combinations of some factors according to this design of experiments are then necessary. Thus, the effect of factors and their interactions, as well as the mathematical modeling of the response, which is the yield of degradation of dyes using the Fenton process of advanced oxidation, make the main objective of this study.

2. Experimental

2.1. Reagents and Experimental Procedure

The dyes cibacron green $C_{60}H_{29}Cl_3N_{16}NiO_{21}S_7 \cdot 6Na$ (CG), methylene blue $C_{16}H_{18}N_3ClS$ (MB), methyl orange $C_{14}H_{14}N_3NaO_3S$ (MO), hydrogen peroxide H_2O_2 (30%, Merck), ferrous sulfate $FeSO_4 \cdot 7H_2O$ (99%, Sigma-Aldrich), sulfuric acid H_2SO_4 (97%, Shanghai Chemical Reagents), HCl (60%, Shanghai Chemical Reagents) and NaCl (99%, Sigma-Aldrich), were used in this work.

The experimental device consisted of a perfectly agitated reactor (reactor batch with a capacity of 600 mL), in which 500 mL of solution was introduced. The aqueous solutions of dye were prepared using distilled water. The pH value of the solution was measured by a pH-meter (Ph 7110-inolab-WTW). The agitation was ensured with a

mechanical stirrer (Janke& Kunkel RW 20). The dye discoloration was made by a Fenton's reagent which consisted of $FeSO_4$ and H_2O_2 mixture. The concentration of the dye in the mixture for a reaction time $t = 60$ min was found by measuring the absorption intensity at 619 nm for CG, 664 nm for MB and 472 nm (pH = 4), 500 nm (pH = 3), 510 nm (pH = 2) for MO. The used cells of the UV/Visible spectrophotometer "SECOMAM-PRIM" were in quartz 1 cm thick. H_2O_2 concentration was measured using the iodide colorimetric method.^{19,20}

The degradation efficiency (Y , %) of dye was determined by Eq. (4):

$$Y = \frac{C_0 - C_t}{C_0} \cdot 100 \quad (4)$$

where C_0 and C_t are the initial concentration of dye (mg/L) at the reaction time t (min).

2.2. The Plackett-Burman Design

2.2.1. Data collection

The Plackett-Burman Design (PBD) of the MINITAB 16 statistical software was used to screen 08 factors in 24 experimental runs in order to follow the oxidative elimination of CG, MO and MB. This design is one of the orthogonal column matrices composed only of the values +1 or -1. The experimental design can be used to get a valid statistical significance test for the factors examined with a minimum number of experiments. Just to consider the factors affecting the response at two levels (+1 and -1), the initial concentration of dye, Fe^{2+} , H_2O_2 and NaCl, pH, the temperature of the solution, the stirring speed, the nature of the acid used to acidify the solution (HCl , H_2SO_4) were studied within the experimental limits of operation, after several preliminary tests. The domain of each factor of the dyes is shown in Table 1.

The effects of different factors in responses and their interactions were analyzed using the variance (ANOVA), this analyzer had included Fisher test (F test), it is associated to the probability (p -value) and the coefficient of determination (R^2) which measures the quality of the model. It consists to identify the significant factors and their corresponding coefficients, so that factors levels can be managed. Large F (>1) and low p -value (<0.05) indicate the good fit of the model to the experimental data.

Table 1. Levels and units of eight operating parameters

Dyes	Level	[Dye] ₀ , mg/L	[Fe ²⁺] ₀ , mg/L	[H ₂ O ₂] ₀ , mg/L	pH	[NaCl] ₀ , mg/L	T , K	V , rpm	Acid
CG	Low (-1)	16.59	2.23	6.12	2	0	290	0	HCl
	High (+1)	73.5	7.26	10.2	4	233.8	318	400	H ₂ SO ₄
MB	Low (-1)	2	0.2	1	2	0	290	0	HCl
	High (+1)	10.42	2	14	4	496	318	400	H ₂ SO ₄
MO	Low (-1)	8	2	1	2	0	290	0	HCl
	High (+1)	28	6	10	4	496	318	400	H ₂ SO ₄

Table 2. Plackett-Burman design matrix of CG discoloration in uncoded units

Run ord.	[H ₂ O ₂] ₀ , mg/L	[Fe ²⁺] ₀ , mg/L	[CG] ₀ , mg/L	T, K	V, rpm	pH	[NaCl] ₀ , mg/L	Acid	Y _{exp} , %	Y _{theor} , %
1	6.12	2.23	73.5	318	400	2	233.8	H ₂ SO ₄	34.60	45.558
2	102	7.26	73.5	290	400	4	0	H ₂ SO ₄	86.84	100.000
3	102	2.23	73.5	290	0	2	233.8	H ₂ SO ₄	76.46	65.567
4	102	2.23	73.5	290	0	2	233.8	H ₂ SO ₄	76.46	65.567
5	6.12	7.26	73.5	318	0	4	233.8	HCl	84.72	84.608
6	102	7.26	16.54	318	400	2	233.8	HCl	79.27	82.916
7	102	7.26	16.54	318	400	2	233.8	HCl	79.27	82.916
8	6.12	7.26	73.5	318	0	4	233.8	HCl	84.52	84.608
9	102	2.23	16.54	290	400	4	233.8	HCl	79.4	75.839
10	102	7.26	16.54	318	0	2	0	H ₂ SO ₄	99.14	95.494
11	102	7.26	16.54	318	0	2	0	H ₂ SO ₄	99.14	95.494
12	102	2.23	73.5	318	0	4	0	HCl	99.46	99.682
13	6.12	2.23	16.54	290	0	2	0	HCl	18.18	32.752
14	6.12	7.26	73.5	290	400	2	0	HCl	60.58	46.053
15	6.12	7.26	16.54	290	0	4	233.8	H ₂ SO ₄	73.33	73.342
16	102	2.23	16.54	290	400	4	233.8	HCl	79.57	75.839
17	6.12	2.23	16.54	318	400	4	0	H ₂ SO ₄	79.3	68.407
18	6.12	2.23	16.54	290	0	2	0	HCl	18.27	32.752
19	102	2.23	73.5	318	0	4	0	HCl	99.88	99.682
20	6.12	7.26	73.5	290	400	2	0	HCl	60.58	46.053
21	102	7.26	73.5	290	400	4	0	H ₂ SO ₄	87.54	100.000
22	6.12	7.26	16.54	290	0	4	233.8	H ₂ SO ₄	73.33	73.342
23	6.12	2.23	16.54	318	400	4	0	H ₂ SO ₄	79.3	68.407
24	6.12	2.23	73.5	318	400	2	233.8	H ₂ SO ₄	34.73	45.558

Table 3. Plackett-Burman design matrix of MO discoloration in un-coded units

Run ord.	[H ₂ O ₂] ₀ , mg/L	pH	[Fe ²⁺] ₀ , mg/L	[MO] ₀ , mg/L	T, K	V, rpm	[NaCl] ₀ , mg/L	Acid	Y _{exp} , %	Y _{theor} , %
1	1	2	6	28	318	0	496	H ₂ SO ₄	53.16	54.7371
2	1	4	2	8	293	400	496	H ₂ SO ₄	79.96	78.1179
3	10	4	6	8	318	400	0	H ₂ SO ₄	93.05	98.4496
4	10	4	2	28	318	0	496	HCl	8.60	11.1654
5	10	2	6	8	293	0	496	H ₂ SO ₄	64.56	63.3579
6	1	4	6	28	293	400	496	HCl	38.54	40.5621
7	1	2	6	28	318	0	496	H ₂ SO ₄	53.87	54.7371
8	10	2	6	8	293	0	496	H ₂ SO ₄	64.60	63.3579
9	1	2	2	28	318	400	0	H ₂ SO ₄	80.19	79.1529
10	1	4	6	8	318	0	0	HCl	66.07	60.8554
11	10	4	2	28	293	0	0	H ₂ SO ₄	8.76	6.4496
12	10	2	2	8	318	400	496	HCl	94.82	92.4896
13	10	4	2	28	293	0	0	H ₂ SO ₄	8.80	6.4496
14	1	4	6	28	293	400	496	HCl	39.09	40.5621
15	1	2	2	8	293	0	0	HCl	44.88	50.1796
16	1	4	2	8	293	400	496	H ₂ SO ₄	79.77	78.1179
17	10	4	6	8	318	400	0	H ₂ SO ₄	93.25	98.4496
18	10	2	6	28	293	400	0	HCl	55.48	50.2179
19	1	2	2	8	293	0	0	HCl	44.88	50.1796
20	1	2	2	28	318	400	0	H ₂ SO ₄	80.56	79.1529
21	10	2	2	8	318	400	496	HCl	94.82	92.4896
22	1	4	6	8	318	0	0	HCl	66.24	60.8554
23	10	2	6	28	293	400	0	HCl	48.45	50.2179
24	10	4	2	28	318	0	496	HCl	9.07	11.1654

Table 4. Plackett-Burman design matrix of MB discoloration in un-coded units

Run ord.	[H ₂ O ₂] ₀ , mg/L	pH	[Fe ²⁺] ₀ , mg/L	[MB] ₀ , mg/L	T, K	V, rpm	[NaCl] ₀ , mg/L	Acid	Y _{exp} , %	Y _{theor} , %
1	1(-1)	4	0.2	2	290	400	496	H ₂ SO ₄	7.20	8.455
2	14(+1)	4	2	2	318	400	0	H ₂ SO ₄	97.11	94.211
3	14(+1)	4	0.2	10.42	290	0	0	H ₂ SO ₄	40.60	50.085
4	14(+1)	2	0.2	2	318	400	496	HCl	18.73	28.155
5	1	4	2	10.42	290	400	496	HCl	43.50	42.480
6	14	2	2	10.42	290	400	0	HCl	24.75	25.320
7	14	4	2	2	318	400	0	H ₂ SO ₄	97.70	94.211
8	1	2	2	10.42	318	0	496	H ₂ SO ₄	28.25	35.730
9	1	4	2	2	318	0	0	HCl	99.13	100.000
10	14	2	0.2	2	318	400	496	HCl	18.73	28.155
11	14	2	2	10.42	290	400	0	HCl	23.60	25.320
12	14	4	0.2	10.42	318	0	496	HCl	96.37	86.945
13	14	2	2	2	290	0	496	H ₂ SO ₄	15.27	7.920
14	14	4	0.2	10.42	318	0	496	HCl	60.58	46.053
15	1	4	2	2	318	0	0	HCl	99.13	100.000
16	1	4	0.2	2	290	400	496	H ₂ SO ₄	7.42	8.455
17	1	2	0.2	2	290	0	0	HCl	2.60	0.000
18	1	2	0.2	2	290	0	0	HCl	2.60	0.000
19	1	2	0.2	10.42	318	400	0	H ₂ SO ₄	26.44	19.105
20	1	2	2	10.42	318	0	496	H ₂ SO ₄	28.46	35.730
21	14	2	2	2	290	0	496	H ₂ SO ₄	15.32	7.920
22	1	4	2	10.42	290	400	496	HCl	43.75	42.480
23	1	2	0.2	10.42	318	400	0	H ₂ SO ₄	26.52	19.105
24	14	4	0.2	10.42	290	0	0	H ₂ SO ₄	40.72	50.085

2.2.2. Data analysis

The value of R^2 is explained as the degree of fitness of the mathematical model with the experimental data, it ranges between 0 and 1. Higher value of R^2 is important. Experimental design, data analysis, plotting of main effects and interactions were performed with MINITAB 16 statistical software. All trials were tested at 95% confidence level. Due to use eight factors, the experimental design will be a matrix of 12 experiments. For more precision, we have duplicated the chosen design, which conducts us to the matrix of 24 trials (Tables 2-4).

3. Results and Discussion

3.1. Variance Analysis of the Results (ANOVA)

Table 5 shows a summary of ANOVA results for MO, CG and MB dyes. The values of p and F as a statisti-

cal indicator to assess which terms of the model are important and highly significant.

Based on the analysis of variance, the highly significant $p = 0.000$ for three dyes, indicates a good regression of the model. The effect of [H₂O₂]₀, pH and [Fe²⁺]₀ on the yield is very strongly significant ($p \leq 0.004$). It is followed by the temperature effect (T), which is also very significant ($p = 0.000$ and $p = 0.012$), in the evaluated experimental range. The positive sign of each factor indicates that the maximum value of these factors results in a higher response than with the minimum value.

The factors which have a negative sign indicate that the minimum value of this factor results in a higher response. The R^2 values of the CG, BM and MO elimination responses obtained in the present study, are 84.14 %, 96.69 % and 98.61 % respectively, all are greater than 80 %. This indicated that only 15.86 %, 3.31 % and 1.39 % of the total dissimilarity might not be explained by the empirical model. According to Joglekar and May²¹ for a good fit of the model, the correlation coefficient should beat a minimum of 80 %.

Table 5. Analysis of variance (ANOVA) of the regression model from the Plackett-Burman design of CG, MB and MO discoloration in coded units

Term	Effect			Coef.			F			p		
	CG	MB	MO	CG	MB	MO	CG	MB	MO	CG	MB	MO
constant				72.661	41.678	67.73	9.94	54.81	132.92	0.000	0.000	0.000
[H ₂ O ₂] ₀	28.41	14.18	-6.91	14.208	7.095	-0.76	35.31	19.50	16.95	0.000	0.001	0.001
pH	22.54	44.81	-15.7	11.271	22.405	-7.88	22.22	194.47	88.06	0.000	0.000	0.000
[Fe ²⁺] ₀	16.05	19.30	8.44	8.027	9.653	2.109	11.27	36.10	25.25	0.004	0.000	0.000
[Dye] ₀	2.406	3.199	-33.5	1.203	1.600	-1.676	0.25	0.99	398.74	0.622	0.335	0.000
T	13.56	38.80	17.99	6.783	19.400	0.720	8.05	145.80	114.86	0.012	0.000	0.000
V	-5.159	-10.78	32.04	-2.580	-5.390	0.080	1.16	11.26	364.16	0.298	0.004	0.000
[NaCl] ₀	-2.713	-13.46	-0.81	-1.356	-6.730	-0.002	0.32	17.55	0.23	0.579	0.001	0.635
Acid	4.706	-11.52	12.47	2.353	-5.760	6.233	0.97	12.85	55.12	0.341	0.003	0.000
Lack of fit							21653.79	4017.0	36.04	0.000	0.000	0.000

Notes : for CG : $R_{CG}^2 = 84.14\%$, $R_{CG}^2(\text{adj}) = 75.67\%$; for MB: $R_{MB}^2 = 96.69\%$, $R_{MB}^2(\text{adj}) = 94.93\%$; for MO: $R_{MO}^2 = 98.61\%$, $R_{MO}^2(\text{adj}) = 97.87\%$

3.2. Mathematical Model Equation

The regression coefficients with the coded units (Table 5) are used in the model equations, representing the relationship between the responses and the studied factors:

$$Y_{CG} = 72.661 + 14.208[H_2O_2]_0 + 11.271pH + 8.027 [Fe^{2+}]_0 + 1.203[CG]_0 + 6.783T - 2.58V - 1.356 [NaCl]_0 + 2.353Acid \quad (5)$$

$$Y_{MB} = 41.678 + 7.095[H_2O_2]_0 + 22.405pH + 9.653[Fe^{2+}]_0 + 1.6[MB]_0 + 19.4T - 5.39V - 6.73[NaCl]_0 - 5.76Acid \quad (6)$$

$$Y_{MO} = 67.73 - 0.768[H_2O_2]_0 - 7.87pH + 2.109 [Fe^{2+}]_0 - 1.676 [MO]_0 + 0.720T + 0.080V - 0.002 [NaCl]_0 + 6.233 Acid \quad (7)$$

3.3. Main Effects Plot

The main effects plot is used to check the difference between the means of one or more factors; it repre-

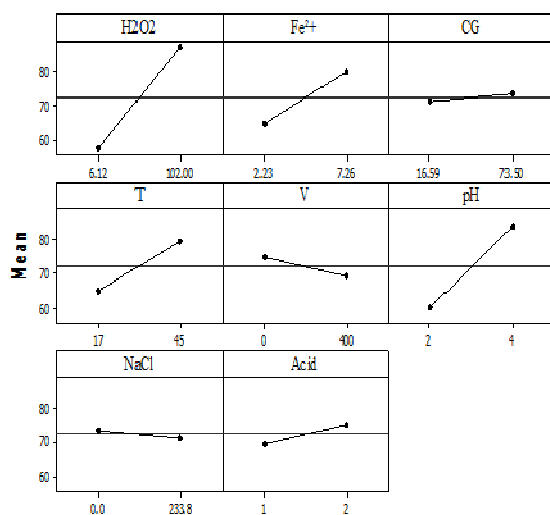


Fig. 1. Main effects plot for CG yield

sents the average response of each level of factor connected by a line. In the case of a two-level factor, the response increases or decreases from a low level to a high one. The difference in the response is the main effect of the factor. To compare the impact of each factor on the degradation efficiency of dyes, the effects of different factors in the form of graphs of the main effects were plotted (Figs. 1-3).

3.4. Interaction Plot for Yield

Interaction diagrams are graphical tools for looking at the interactions or dependencies between factors. If the effect of one process parameter depends on the level of the other parameters, the interaction will occur.

The absence of interaction graphically is showed by parallels, if there is an interaction effect, the two lines will intersect each other.¹⁸ Figs. 4-6 illustrate the interaction plot for discoloration yield of three dyes.

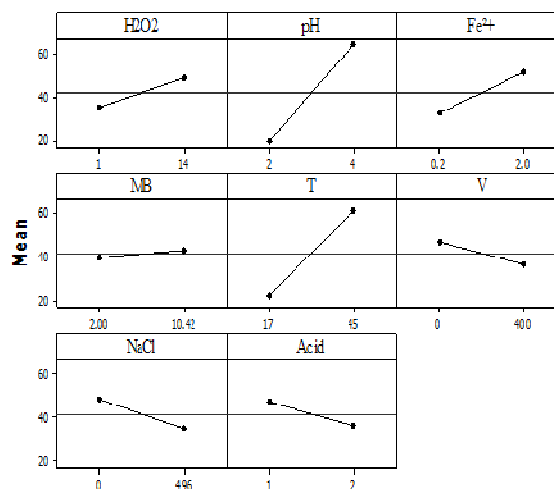


Fig. 2. Main effects plot for MB yield

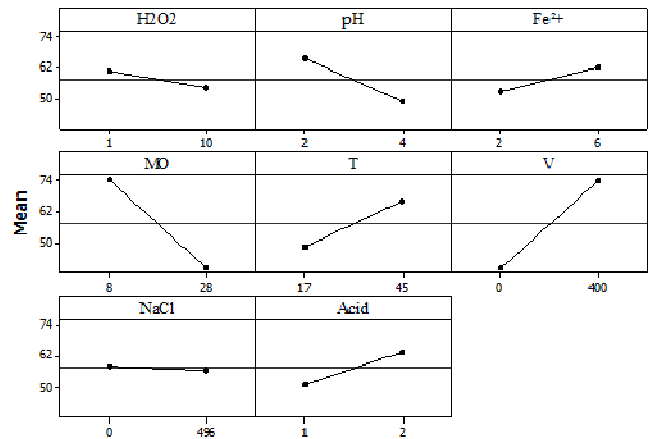


Fig.3. Main effects plot for MO yield

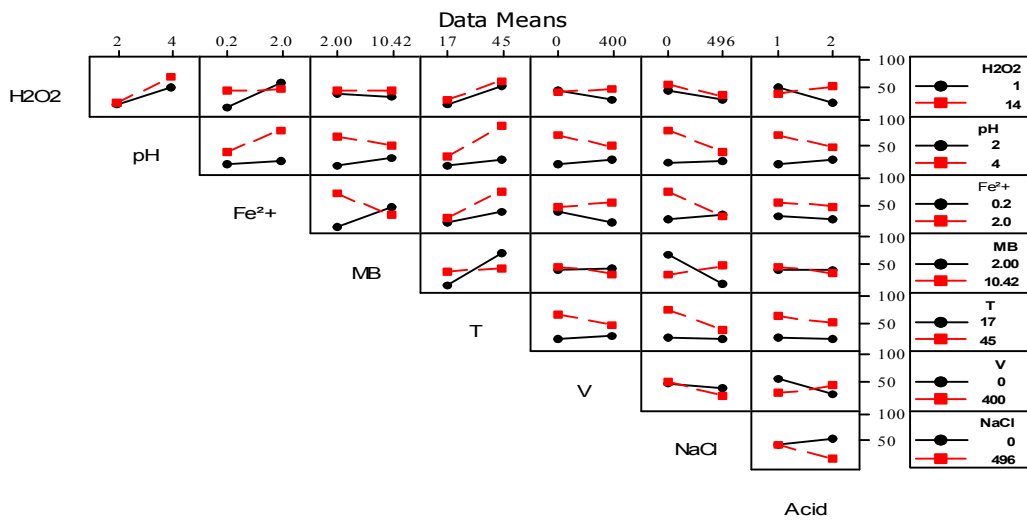


Fig. 4. Interaction plot for MB yield

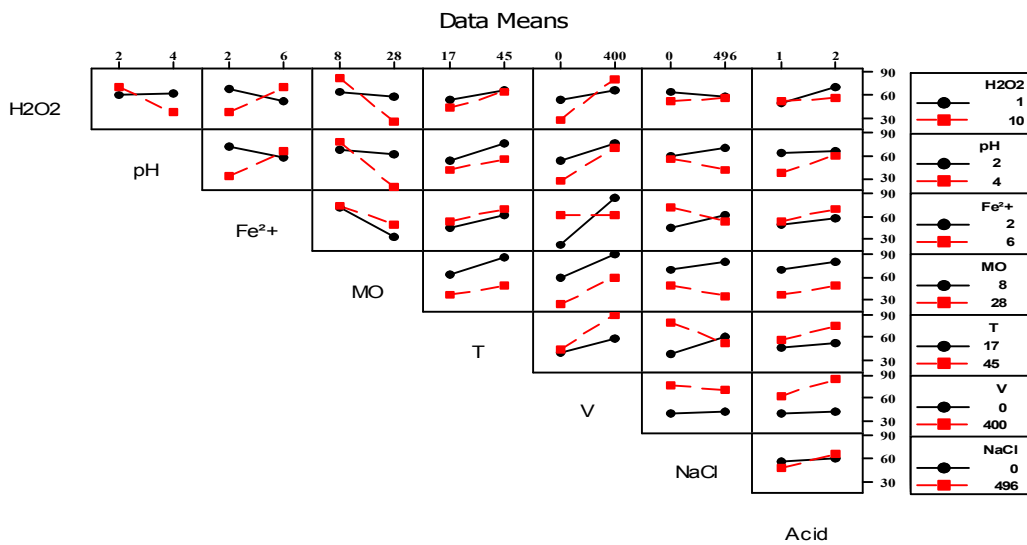


Fig. 5. Interaction plot for MO yield

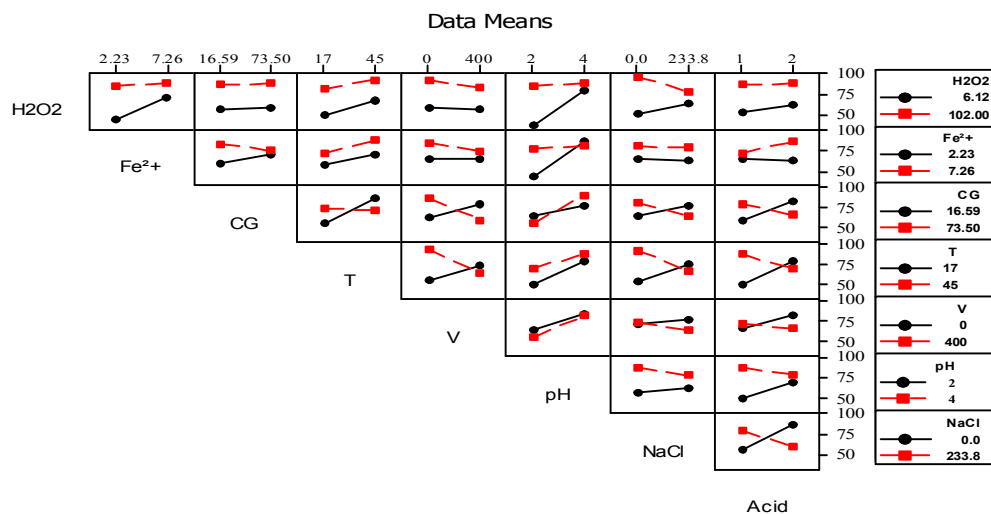
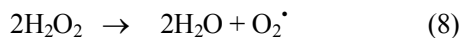


Fig. 6. Interaction plot for CG yield

3.5. Interpretation of the Results Obtained from Various Diagrams

Effect of initial H₂O₂ concentration

The degradation efficiency of dyes (CG and MB) increases when [H₂O₂]₀ is high (Figs. 1, 2), because hydrogen peroxide is the source of hydroxyl radicals, responsible for the degradation of organic material, therefore the probability of contact between dyes molecules with the free hydroxyl radicals increases. However, the efficiency of MO degradation decreases when [H₂O₂]₀ increases (Fig. 3), interactions were observed with all the parameters studied “line 1” (Fig. 5). This is due to the scavenging of [•]OH by an excess of H₂O₂ which conducts to the generation of radicals less reactive like HOO[•], its oxidation potential too is lower than [•]OH,²² as shown below:



In addition, the excess of H₂O₂ reacts with ferric ions to form a hydroperoxyl radicals²³ according to Eq. (10):



Effect of pH

The discoloration of MO at pH = 2-4 has a significant negative effect (Fig. 3); therefore the optimum pH is between 2 and 4, this is confirmed by the studies of Luo²⁴ and Youssef,²⁵ who have noticed that the optimum pH values for MO degradation were reached at 2.5 and 2.7, as well as pH interacted with [H₂O₂]₀ and [Fe²⁺]₀ (Fig. 5); on the other hand for MB and CG the pH value has a very important positive effect (Figs. 1, 2) and an interaction with the [H₂O₂]₀ (Figs. 4, 6). Therefore pH = 4 favors the discoloration yield of these two dyes.

Effect of the initial concentration of [Fe²⁺]₀

The discoloration yield of the three dyes (CG, MO and MB) increases when [Fe²⁺]₀ is higher in the selected range (Figs. 1-3). These results are in agreement with those of Hashemian *et al.*²⁶ and Sun,⁷ who also observed that the rate of degradation enhances once the concentration of ferrous ions increases. Indeed, more hydroxyl radicals HO[•] are produced when [Fe²⁺]₀ increases according to Eq. (1).

So Fe²⁺ has a very important effect to trigger the decompositions of H₂O₂ in order to generate HO[•] in the Fenton process.

Effect of the initial dye concentration

Another important parameter that may affect the rate of degradation, is the initial concentration of organic dyes. The effects of [MB]₀ and [CG]₀ have a powerless positive impact on the discoloration yield of the two dyes (Figs. 1, 3). This can be explained by the increasing of the frequency of collisions between reactants when their concentration increases. Thus, the frequency of effective collisions that cause a reaction will be also high. Increasing the amount of dye molecules per unit of volume increases the probability of collision between organic material and OH₂, this conducted to increase the efficiency of discoloration.²⁷ However, the effect is negative for MO (Fig. 3), this is due to the strong interaction with [H₂O₂]₀ (Fig. 5) which has a negative effect because its excess in the solution leads to the generation of [•]OOH less reactive than [•]OH (Eqs. 8, 9) which strongly and negatively influences the yield.

Effect of the solution temperature

The temperature has a very important positive effect on discoloration efficiency of three dyes (Figs. 1-3). When the temperature increases, the reaction velocity increases between ferrous ions and H₂O₂, this phenomenon causes the generation of hydroxyl radicals.²⁸

In addition, a higher temperature could provide more energy for the reactive molecules to overcome the activation energy of the reaction.²⁹ We can observe interactions between temperature and $[MB]_0$, $[CG]_0$ (Figs. 4, 6) but for MO, only one interaction with $[H_2O_2]_0$ can be seen (Fig. 5). However, carrying out the reaction at a temperature above 318 K may decrease the discoloration yield. Generally, a higher temperature could have an influence on the decomposition of H_2O_2 into water and oxygen.

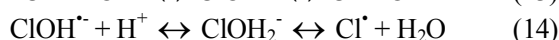
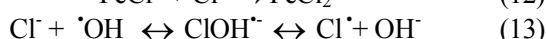
Effect of stirring speed

It is observed from Figs. 1 and 2 that the stirring speed (V) has a negative effect against the elimination of CG and MB, these observations can be explained by the interaction of the effect of the dye concentration and the temperature (Figs. 4, 6), both factors neglected the effect of stirring speed.

But when the speed reached 400 rpm, a positive effect on discoloration of MO was observed which can be explained by the strong interaction between $[H_2O_2]_0$ and $[Fe^{2+}]_0$ (Fig. 5), thus $[H_2O_2]_0$ has a negative effect on the yield and the stirring speed has a positive effect to promote the contact of reactants and also affects the mass transfer between the chemical species.

Effect of initial salt concentration $[NaCl]_0$

The discoloration of three dyes mentioned above that $[NaCl]_0$ has no effect on the degradation of CG and MO in the experiment range (Figs. 1, 3), so it can be explained that the addition of a higher concentration of ferrous ions could break the inhibition from chloride ions. It means, there is a strong interaction between $[NaCl]_0$ and $[Fe^{2+}]_0$ (Fig. 5). On the other hand, the methylene blue has a negative effect when $[NaCl]_0$ increases from 0 to 496 ppm. This is due to the strong interaction between $[Fe^{2+}]_0$ and $[MB]_0$ (Fig. 4): the interaction of chloride with Fe^{2+} ions can produce complex chemicals according to Eqs. 11, 12 or scavenger of hydroxyl radicals (Eqs. 13, 14):^{30,31}



Another interpretation may explain that the interaction between $[NaCl]_0$ and $[MB]_0$ is due to the increased degree of aggregation of the ionic dye in water. Sometimes it is referred as a "common ionic effect", which can greatly limit the solubility and ionization of dyes and the lower ability of dye molecules to react with hydroxyl radicals.³² Therefore, the addition of sodium chloride can reduce the electrostatic repulsive forces between the dye anions which increase the tendency for the dye species to aggregate.³³

Effect of the acid nature used to acidify the solution

Generally, the anions Cl^- and SO_4^{2-} commonly coexist with dyes in wastewater. The using of acids like H_2SO_4 enhances the discoloration efficiency of CG and MO solutions (Figs. 1, 3). On the other hand, the discoloration of the MB solution is favored by hydrochloric acid (Fig. 2). However, it is advisable to use sulfuric acid because it corresponds to the iron salt used avoiding the formation of complex compounds.

4. Conclusions

The results of the eight-factor interactions showed the relation between these parameters, but there was a difference in the degree of influence of the studied effects because it depends on the structure of organic dyes, so each dye has a self-structure (types of hydroxyl substituent and their position, the length of the main chain, *etc.*), as well as the choice of the limits of the factors that may cause a risk of not showing the effect of factors, if the levels are too close or too far from each other.

ANOVA analysis of variance gave the signification or non-signification of the factors; the p -value of 0.000 for three pollutants indicated the good regression of the model. The linear regression was compared between the values of the theoretical efficiency given by the mathematical model and the values of the experimental yield. Indeed, the adjustment was almost perfect as the correlation constant was equal to 0.9861, 0.9669 and 0.8414 for MO, MB and CG, respectively.

The concentrations of hydrogen peroxide and Fe^{2+} , pH and temperature are the most important factors to promote the efficiency of the reaction (p -value was very significant for these three dyes). However, the key factor for the Fenton reaction was the $[H_2O_2]_0$, because it had an effect of interaction with all the factors. The variation of this concentration varies the effect of other factors and the efficiency of the reaction: it is the origin of the hydroxyl radicals, however, more H_2O_2 may conduct to reduce the degradation of the pollutant, this is the case of MO oxidation. The application of the Plackett-Burman design (PBD) has proven to be an efficient and rapid method to identify the most critical factors that influence the degradation of three dyes, their interaction, and the quality of the Fenton process.

References

- [1] Fenton, H.J.H., Jackson, H.J. I. – The Oxidation of Polyhydric Alcohols in Presence of Iron. *J. Chem. Soc. Trans.* **1899**, 75, 1-11. <https://doi.org/10.1039/CT8997500001>

- [2] Fenton, H.J.H., Jones, H.O. VII. – The Oxidation of Organic Acids in Presence of Ferrous Iron. Part I. *J. Chem. Soc. Trans.* **1900**, 77, 69-76. <https://doi.org/10.1039/CT9007700069>
- [3] Li, W.; Xu, L. Research Methods for the Degradation Mechanism of Organic Pollutants in Wastewater. *Acta Chim. Sinica* **2019**, 77, 705-716. <https://doi.org/10.6023/A19030073>
- [4] Su, S.; Liu, Y.; Liu X.; Jin, W.; Zhao, Y. Transformation Pathway and Degradation Mechanism of Methylene Blue Through B-Feooh@GO Catalyzed Photo-Fenton-Like System. *Chemosphere* **2019**, 218, 83-92. <https://doi.org/10.1016/j.chemosphere.2018.11.098>
- [5] Jegan Durai, N.; Gopalakrishna, G.V. T.; Padmanaban, V.C.; Selvaraju N. Oxidative Removal of Stabilized Landfill Leachate by Fenton's Process: Process Modeling, Optimization & Analysis of Degraded Products. *RCS Adv.* **2020**, 10, 3916-3925. <https://doi.org/10.1039/C9RA09415F>
- [6] Elhalil, A.; Tounsadi, H.; Elmoubarki R.; Mahjoubi, F.Z.; Farnane M.; Sadiq, M.; Abdennouri, M.; Qourzal, S.;Barka, N. Factorial Experimental Design for The Optimization of Catalytic Degradation of Malachite Green Dye in Aqueous Solution by Fenton Process. *Water Resour. Ind.* **2016**, 15, 41-48. <https://doi.org/10.1016/j.wri.2016.07.002>
- [7] Jian-Hui Sun, J.-H.; Sun S.-P.; Wang G.-L.; Qiao L.-P. Degradation of Azo Dye Amido Black 10B in Aqueous Solution by Fenton Oxidation Process. *Dyes Pigm.* **2007**, 74, 647-652. <https://doi.org/10.1016/j.dyepig.2006.04.006>
- [8] Sillanpää, M., Ncibi, M.C., Matilainen, A. Advanced Oxidation Processes for The Removal of Natural Organic Matter from Drinking Water Sources: A Comprehensive Review. *J. Environ. Manage.* **2018**, 208, 56-76. <https://doi.org/10.1016/j.jenvman.2017.12.009>
- [9] Khue, D.N.; Lam, T.D.; Van Chat, N.; Bach, V.Q.; Minch, D.B.; Loi, V.D.; Van Anh, N. Simultaneous Degradation of 2,4,6-Trinitrophenyl-N-Methylnitramine (Tetryl) and Hexahydro-1,3,5-Trinitro-1,3,5 Triazine (RDX) in Polluted Wastewater Using Some Advanced Oxidation Processes. *J. Ind. Eng. Chem.* **2014**, 20, 1468-1475. <https://doi.org/10.1016/j.jiec.2013.07.033>
- [10] Oh, S.Y.; Yoon, H.S.; Jeong, T.Y.; Kim, S.D. Evaluation of Remediation Processes for Explosive-Contaminated Soils: Kinetics and Microtox[®] Bioassay. *J. Chem. Technol. Biotechnol.* **2016**, 91, 928-937. <https://doi.org/10.1002/jctb.4658>
- [11] Ghernaout, D.; Elboughdiri, N.; Ghareba, S. Fenton Technology for Wastewater Treatment: Dares and Trends. *OALib. J.* **2020**, 7, e6045. <https://doi.org/10.4236/oalib.1106045>
- [12] Karthikeyan, S.; Titus, A.; Gnanamani, A.; Mandal, A.B.; Sekaran, G. Treatment of Textile Wastewater by Homogeneous and Heterogeneous Fenton Oxidation Processes. *Desalination* **2011**, 281, 438-445. <https://doi.org/10.1016/j.desal.2011.08.019>
- [13] Hermosilla, D.; Merayo, N.; Gascó, A.; Blanco, Á. The Application of Advanced Oxidation Technologies to The Treatment of Effluents from The Pulp and Paper Industry: A Review. *Environ. Sci. Pollut. Res.* **2015**, 22, 168-191. <https://doi.org/10.1007/s11356-014-3516-1>
- [14] Ma, C.; Feng, S.; Zhou, J.; Chen, R.; Wei, Y.; Liu, X.; Wang, S. Enhancement of H₂O₂ Decomposition Efficiency by The Co-Catalytic Effect of Iron Phosphide on The Fenton Reaction for The Degradation of Methylene Blue. *Appl. Catal. B* **2019**, 259, 118015. <https://doi.org/10.1016/j.apcatb.2019.118015>
- [15] Munoz, M.; De Pedro, Z.M.; Casas, J.A.; Rodriguez, J.J. Preparation of Magnetite-Based Catalysts and Their Application in Heterogeneous Fenton Oxidation – A Review. *Appl. Catal. B* **2015**, 176-177, 249-265. <https://doi.org/10.1016/j.apcatb.2015.04.003>
- [16] Pan, X.; Cheng, S.; Su, T.; Zuo, G.; Zhao, W.; Qi, X.; Wei, W.; Dong, W. Fenton-Like Catalyst Fe₃O₄@Polydopamine-MnO₂ for Enhancing Removal of Methylene Blue in Wastewater. *Colloids Surf. B* **2019**, 181, 226-233. <https://doi.org/10.1016/j.colsurfb.2019.05.048>
- [17] Esmaeili, N.; Mohammadi, P.; Abbaszadeh, M.; Sheibani, H. Au Nanoparticles Decorated on Magnetic Nanocomposite (GO-Fe₃O₄/Dop/Au) as A Recoverable Catalyst for Degradation of Methylene Blue and Methyl Orange in Water. *Int. J. Hydrog. Energy* **2019**, 44, 23002-23009. <https://doi.org/10.1016/j.ijhydene.2019.07.025>
- [18] Antony, J. 3 - Understanding Key Interactions in Processes. *Design of Experiments for Engineers and Scientists*, 2nd ed.; Elsevier, 2014, pp 19-32. <https://doi.org/10.1016/B978-0-08-099417-8.00003-1>
- [19] Iida, Y.; Yasui, K.; Tuziuti, T.; Sivakumar M. Sonochemistry and Its Dosimetry. *Microchem. J.* **2005**, 80, 159-164. <https://doi.org/10.1016/j.microc.2004.07.016>
- [20] Ge, J.; Qu, J.: Degradation of Azo Dye Acid Red B on Manganese Dioxide in The Absence and Presence of Ultrasonic Irradiation. *J. Hazard Mater.* **2003**, 100, 197-207. [https://doi.org/10.1016/S0304-3894\(03\)00105-5](https://doi.org/10.1016/S0304-3894(03)00105-5)
- [21] Joglekar, A.M.; May, A.T. Product Excellence Through Design of Experiments. *Cereal Foods World* 1987, **32**, 857-868.
- [22] Buxton, G.V.; Greenstock, C.L.; Helman, W.P.; Ross A.B. Critical Review of Rate Constants for Reactions of Hydrated Electrons, Hydrogen Atoms and Hydroxyl Radicals (Oh/O–) in Aqueous Solution. *J. Phys. Chem. Ref. Data* 1988, 17, 513. <https://doi.org/10.1063/1.555805>
- [23] Kavitha, V.; Palanivelu, K. Destruction of Cresols by Fenton Oxidation Process. *Water Res.* **2005**, 39, 3062-3072. <https://doi.org/10.1016/j.watres.2005.05.011>
- [24] Luo, W.; Abbas, M.E.; Zhu, L.; Deng, K.; Tang, H. Rapid Quantitative Determination of Hydrogen Peroxide by Oxidation Decolorization of Methyl Orange Using a Fenton Reaction System. *Anal. Chim. Acta* **2008**, 629(1-2), 1-5. <https://doi.org/10.1016/j.aca.2008.09.009>
- [25] Youssef, N.A.; Shaban, S.A.; Ibrahim, F.A.; Mahmoud, A.S. Degradation of Methyl Orange Using Fenton Catalytic Reaction. *Egypt. J. Pet.* **2016**, 25, 317-321. <https://doi.org/10.1016/j.ejpe.2015.07.017>
- [26] Hashemian, S.; Tabatabae, M.; Gafari, M. Fenton Oxidation of Methyl Violet in Aqueous Solution. *J. Chem.* **2013**, 2013, Article ID 509097. <https://doi.org/10.1155/2013/509097>
- [27] Hashemian, S. Fenton-Like Oxidation of Malachite Green Solutions: Kinetic and Thermodynamic Study. *J. Chem.* **2013**, 2013, Article ID 809318. <https://doi.org/10.1155/2013/809318>
- [28] de Souza, D.R.; Mendonça Duarte, E.T.F.; de Souza Girardi, G.; Velani, V.; da Hora Machado, A.E.; Sattler, C.; de Oliveira, L.; de Miranda, J.A. Study of Kinetic Parameters Related to The Degradation of an Industrial Effluent Using Fenton-Like Reactions. *J. Photochem. Photobiol. A* **2006**, 179, 269. <https://doi.org/10.1016/j.jphotochem.2005.08.025>

- [29] Xu, H.Y.; Prasad, M.; Liu, Y. Schorl: A Novel Catalyst in Mineral-Catalyzed Fenton-Like System for Dyeing Wastewater Discoloration. *J. Hazard. Mater.* **2009**, *165*, 1186-1192. <https://doi.org/10.1016/j.jhazmat.2008.10.108>
- [30] Sirtori, C.; Zapata, A.; Oller, I.; Gerniak, W.; Agüera, A.; Malato, S. Solar Photo-Fenton as Finishing Step for Biological Treatment of a Pharmaceutical Wastewater. *Environ. Sci. Technol.* **2009**, *43*, 1185-1191. <https://doi.org/10.1021/es802550y>
- [31] Bacardit, J.; Stötzner, J.; Chamorro E.; Esplugas, S. Effect of Salinity on the Photo-Fenton Process. *Ind. Eng. Chem.Res.* **2007**, *46*, 7615-7619. <https://doi.org/10.1021/ie070154o>
- [32] Dong, Y.; Chen, J.; Li, C.; Zhu, H. Decoloration of Three Azo Dyes in Water by Photocatalysis of Fe(III)-Oxalate Complexes/H₂O₂ in the Presence of Inorganic Salts. *Dyes Pigm.* **2007**, *73*, 261-268. <https://doi.org/10.1016/j.dyepig.2005.12.007>
- [33] El-Fass, M.M.; Badawy, N.A.; El-Bayaa, A.A.; Moursy, N.S. The Influence of Simple Electrolyte on the Behaviour of Some Acid Dyes in Aqueous Media. *Bull. Korean Chem. Soc.* **1995**, *16*(5), 458-461.

Received: February 08, 2021 / Revised: February 15, 2021 /
Accepted: June 04, 2021

ЕФЕКТ ВЗАЄМОДІЇ РОБОЧИХ ПАРАМЕТРІВ ПРИ ОКИСНЕННІ РЕАГЕНТОМ ФЕНТОНА РІЗНИХ БАРВНИКІВ. ЗАСТОСУВАННЯ МЕТОДУ ПЛАКЕТТА–БЕРМАНА

Анотація. Вивчено ефект взаємодії між вісьмома робочими параметрами, які можуть істотно впливати на деградацію трьох органічних барвників, що мають різну структуру (Сіваcron зелений, метиленовий синій і метилоранж). Оцінювання ефекту виконано статистично за допомогою скринінгового методу Плакетта-Бермана. Придатність моделі перевірено з визначенням коефіцієнта R^2 . Проаналізовано та проілюстровано параметри процесу, які вплинули на ефективність деградації барвників; найважливіші значення (p та F) для трьох барвників довели придатність моделі. Показано, що отримані результати взаємодії параметрів дають можливість виділити ключовий фактор для підвищення ефективності процесу Фентона.

Ключові слова: окиснення Фентона, видалення барвників, оброблення води, дизайн експерименту, аналіз ANOVA.